



The new soluble tetra-substituted oxo-titanium phthalocyanines: Synthesis, characterization, spectral and colorimetric pH sensing properties

Ebru Yabaş

Sivas Cumhuriyet University, Advanced Technology Application and Research Center, 58140, Sivas, Türkiye



ARTICLE INFO

Article history:

Received 3 July 2022

Revised 21 March 2023

Accepted 25 March 2023

Available online 26 March 2023

Keywords:

Phthalocyanine

Titanium

UV-Vis

pH sensor

Fluorescence

SEM

ABSTRACT

New imidazole tetrasubstituted oxo-titanium phthalocyanine **1** was synthesized by tetramerization reaction of imidazole substituted phthalonitrile in the presence of titanium(IV) butoxide. N-alkylated imidazole tetrasubstituted oxo-titanium phthalocyanine **2** was prepared by N-alkylation reaction of compound **1** with iodomethane in basic medium. Afterwards, as a result of the quaternization reaction of compound **2**, water-soluble oxo-titanium phthalocyanine **3** was prepared. The synthesized compounds were characterized by UV-Vis, FT-IR, ¹H-NMR, MALDI-TOF MS and elemental analysis. The spectral properties, surface morphologies in powder form and thin films, colorimetric pH sensing properties and aggregation behaviors of the synthesized compounds were investigated. We also used the UV-Vis spectroscopy technique to experimentally find the optical band gap of compound **1** with the best thin-film surface properties. In this context, transmittance, absorption and band gap energy of compound **1** thin film were investigated.

© 2023 Elsevier B.V. All rights reserved.

1. Introduction

Phthalocyanines are organic semiconductor materials with excellent stability to heat, light, moisture and oxygen. Their absorption spectra have strong absorption bands (Q- and B-bands) in the 400 nm and 800 nm range caused by the $\pi-\pi^*$ transitions of the 18π electron conjugate system. The characteristic Q band of phthalocyanines is due to the transition of the Pc ring from the Highest Filled Molecular Orbital (HOMO) to the Lowest Filled Molecular Orbital (LUMO) $\pi-\pi^*$, while the characteristic B band is due to the deep $\pi-\pi^*$ transitions [1]. In addition, phthalocyanine compounds attract attention in many applications due to their strong absorbance at high wavelength, high fluorescent quantum yields and long wave excitation and emission maxima, especially in the near infrared region (NIR) [2–4]. Increasing the conjugation of phthalocyanines with substituted groups in their structure may shift the absorption of phthalocyanines further into the red region. However, this reduces the solubility of the molecule. For this, it may be preferable to use a metal such as titanium (Ti), which causes the Q-band to redshift a little more in the structure. It is also known that oxo-titanium phthalocyanine compounds show rich spectroscopic and photophysical properties [4]. The spectro-

scopic study of metallophthalocyanines gives very useful information about charge transfer between the central metal and the phthalocyanine ligand. Optical band gap of the organic semiconductors is an important issue, for applications such as light emitting diode (LED), organic photovoltaic devices (OPV) and the photodynamic therapy (PDT) as a photosensitizer [5]. One of the easiest ways to determine the optical energy band gap of the material is to use the absorption spectra [5]. On the other hand, there is increasing interest in the development of basic electronic devices such as pH sensitive sensors and molecular switches. In the literature, there are many studies on the pH sensing properties of imidazole derivatives [6–11]. In the past years, we have carried out studies in our laboratory on the synthesis of different imidazole substituted phthalocyanine derivatives and the investigation of their electrical, electrochemical and gas sensor properties [12–14]. When we look at the literature, we see that imidazole substituted phthalocyanine compounds have been examined in a few reports [15–25]. In our study, imidazole tetrasubstituted oxo-titanium phthalocyanine compound was synthesized as a successful pH sensing molecule and its derivatives were prepared by N-alkylation and quaternization reactions. To the best of our knowledge, the colorimetric pH sensing properties of synthesized imidazole substituted phthalocyanine compounds were observed for the first time in this study. The spectral properties of the prepared compounds were also investigated.

E-mail address: eyabas@cumhuriyet.edu.tr

2. Experimental

2.1. General

All solvents used in the reactions were dried by special methods and over molecular sieve [26] and all reactions were carried out under argon gas. The imidazole substituted phthalonitrile derivative, which is the starting material, was synthesized according to the literature [12]. UV-Vis spectra were recorded on a Shimadzu UV-1800 UV-Vis spectrophotometer. Optical characterization was carried out using Cary 5000 UV-Vis-NIR spectrophotometer. Fluorescence spectra of compounds were taken with Shimadzu RF 5301 fluorescence spectrophotometer. ¹H-NMR spectra were measured on a 400 MHz NMR spectrometer. FT-IR spectra were measured by preparing a KBr pellet on an AT1 Unicam-Mattson 1000 spectrometer. The surface morphology of powder form and thin films of compounds were examined with a TESCAN® MIRA3 XMU scanning electron microscope. Melting points were determined with the Electrothermal 9100 melting point detector.

2.2. Synthesis of compounds

2.2.1. Compound 1

A solution of a mixture of imidazole substituted phthalonitrile (100.0 mg, 0.26 mmol) and titanium(IV) butoxide (18.0 mg, 0.052 mmol) in N,N-dimethylformamide (DMF):pentanol (1:3) (2 mL) was heated at 180°C in the presence of 1,8-diazabicyclo[5.4.0]undec-7-ene (DBU) for 20 hours. The resulting mixture was precipitated with ether (10 mL), filtered and dried. The green solid was washed sequentially with methanol (MeOH) (2 × 5 mL) and acetone (3 × 5 mL) and dried in vacuum. The resulting dark green solid was soluble in tetrahydrofuran (THF), DMF and dimethyl sulfoxide (DMSO). Yield: 64% (52.0 mg). M.p.: >300°C. ¹H-NMR (400 MHz, DMSO-d₆, 25°C), (δ: ppm): 13.4 (br s, 4H, Im-NH, disappeared on D₂O addition); 9.0-7.0 (br m, 52H, Ar-H). UV-Vis (DMSO) λ_{max}/nm (log ε, dm³mol⁻¹cm⁻¹): 705 (5.35), 638 (4.46), 350 (5.22). FT-IR (KBr pellet) ν (cm⁻¹): 3165; 3093; 1621; 1489; 767; 694. MS (MALDI-TOF) m/z: 1596 [M+H₂O+H]⁺. Anal.Calc. for C₉₂H₅₆N₁₆S₄O₄Ti: C, 70.04; H, 3.58; N, 14.21; S, 8.13%. Found: C, 70.21; H, 3.75; N, 14.39; S, 8.46%.

2.2.2. Compound 2

Compound 1 (100.0 mg, 0.06 mmol) was dissolved in DMF (3 mL), iodomethane CH₃I (34.0 mg, 0.25 mmol) was added, and then stirred in the presence of potassium carbonate (K₂CO₃) (41.5 mg, 0.30 mmol) for 8 hours at room temperature. The reaction solvent was evaporated under reduced pressure, and then the crude residue was dissolved in chloroform (CHCl₃) and filtered. The solution was concentrated and precipitated by adding n-hexane, filtered and dried in vacuum. The dark green solid was soluble in CHCl₃, acetone, MeOH, THF, DMF and DMSO. Yield: 79% (92.0 mg). M.p.: >300°C. ¹H-NMR (400 MHz, CDCl₃, 25°C), (δ: ppm): 8.8-7.0 (br m, 52H, Ar-H), 1.5 (s, 12H, Aliphatic-H). UV-Vis (DMSO) λ_{max}/nm (log ε, dm³mol⁻¹cm⁻¹): 701 (5.11), 635 (4.35), 359 (4.86). FT-IR (KBr pellet) ν (cm⁻¹): 2864; 1608; 1486; 765; 696. Anal.Calc. for C₉₆H₆₄N₁₆S₄O₄Ti: C, 70.51; H, 3.95; N, 13.72; S, 7.85%. Found: C, 70.60; H, 4.07; N, 13.90; S, 7.91%.

2.2.3. Compound 3

A mixture of compound 2 (50.0 mg) and iodoethane (CH₃CH₂I) (0.1 mL) was stirred in THF (1 mL) at room temperature for 10 hours. The resulting mixture was precipitated with ether, filtered and dried. The dark green solid was soluble in H₂O. Yield: 83% (45.0 mg). M.p.: >300°C. UV-Vis (H₂O) λ_{max}/nm (log ε,

dm³mol⁻¹cm⁻¹): 713 (4.71), 668 (4.30), 372 (5.34). FT-IR (KBr pellet) ν (cm⁻¹): 2929; 2856; 1644; 1599; 1488; 765; 698. Anal.Calc. for C₁₀₄H₈₄N₁₆S₄O₄Ti: C, 55.33; H, 3.75; N, 9.93; S, 5.68%. Found: C, 55.97; H, 3.99; N, 10.11; S, 5.88%.

2.3. Preparation of organic thin films

To prepare the thin films, firstly the compounds were separately dissolved in THF. Then, the prepared solutions were dropped on the glass surfaces and dried at room temperature.

2.4. Fluorescence measurements

Fluorescence quantum yields were calculated according to the following equation by taking fluorescence measurements of phthalocyanine solutions prepared using spectroscopic grade DMSO as solvent:

$$\Phi_F = \Phi_F(\text{Std}) \frac{F A_{\text{Std}} \eta^2}{F_{\text{Std}} \eta_{\text{Std}}^2}$$

where F and F_{Std} are the areas under the fluorescence emission curves of the compound and the ZnPc standard, respectively. A and A_{Std} are the absorbance of the samples and ZnPc standard at the excitation wavelength, respectively, η and η_{Std} are the refractive indexes of solvents used for compound and ZnPc standard, respectively. Unsubstituted ZnPc was used as standard (Φ_F = 0.18 in DMSO) [27].

3. Results and discussions

3.1. Synthesis and characterization

The synthesis routes of compounds 1-3 are shown in Fig. 1. As summarized in the figure, substituted oxo-titanium phthalocyanine 1 was synthesized as a result of the tetramerization reaction of the phthalonitrile derivative by utilizing the template effect of the metal. Then, N-alkylated substituted oxo-titanium phthalocyanine 2 was synthesized by the alkylation of the imidazole-NH group on the substituents of compound 1 in basic medium. Finally, water soluble oxo-titanium phthalocyanine compound 3 was synthesized by the quaternization reaction of compound 2 with iodoethane. In addition, the fact that compound 3 is easily soluble in water indicates that the quaternization reaction has taken place. The synthesized compounds were purified by utilizing the solubility differences in different solvents. The purified compounds 1-3 were obtained in very high yields of 64%, 79% and 83%, respectively. Compounds were characterized by UV-Vis, FT-IR, ¹H-NMR, MALDI-TOF MS and elemental analysis.

In the FT-IR spectrum of compound 1, it was observed that the sharp -C≡N characteristic vibration band, which appeared at 2233 cm⁻¹ of the phthalonitrile compound used in the synthesis of compound 1, disappeared. This indicates that the tetramerization reaction took place and the product was formed. Also, broad peaks in the range of 3165-3093 cm⁻¹ belonging to the imidazole-NH groups are observed in the FT-IR spectrum of compound 1. These peaks disappeared in the FT-IR spectrum of compound 2 as a result of the N-alkylation reaction. These peaks were also not observed in the FT-IR spectrum of compound 3. In addition, peaks of 2864 cm⁻¹ and 2929-2856 cm⁻¹ of alkyl groups were observed in the FT-IR spectra of compounds 2 and 3, respectively. This confirms that the N-alkylation and quaternization reactions have taken place [12,13].

In the ¹H-NMR spectra of compounds 1 and 2, aromatic-H peaks were observed as wide multiplet peaks in the range of 9.0-7.0 ppm. In the ¹H-NMR spectrum of compound 1, the peak belonging to the imidazole -NH group was observed broadly at 13.4

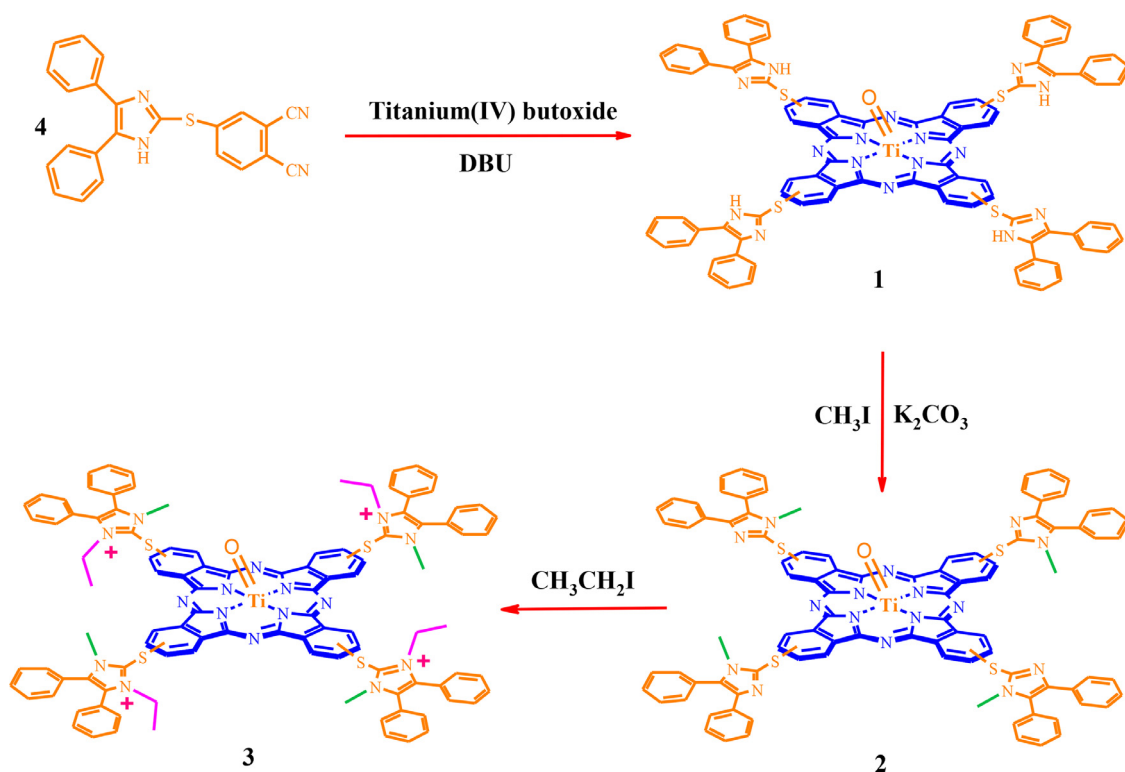


Fig. 1. Synthesis of oxo-titanium phthalocyanine compounds 1-3.

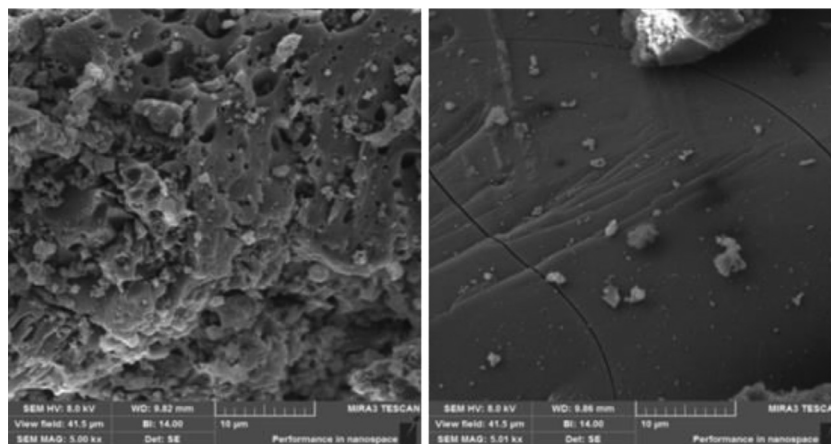


Fig. 2. SEM image of inside and outside of compound 1.

ppm, while this peak disappeared in the $^1\text{H-NMR}$ spectrum of compound **2**. This difference observed in the spectra proves that the N-alkylation reaction takes place over the $-\text{NH}$ group. In addition, the peak of the $-\text{CH}_3$ group observed at 1.5 ppm in the $^1\text{H-NMR}$ spectrum of compound **2** indicates that the N-alkylation reaction has taken place [12,13]. The integral ratios of the peaks are also compatible with the structure of the compounds. The elemental analysis results of the compounds **1-3** are in agreement with the theoretically calculated values.

3.2. SEM images

SEM investigation was conducted at 10kV and 10 mm working distance with Tescan Mira3 XMU (Brno, Czechia). Gold coating was done with magnetron sputtering device named as Q150RES for 3 min. to be 5 nm of gold surface. The powder form SEM image of compound **2** was seen in Fig. 2. As the crushed inner side of compound **1** was evaluated, the sudden precipitation produces many

inner bubbles, seen as pores; moreover, the brittle structure as seen from inside as well as outside by low energetic cracks and layer-like structure is evident (Fig. 2). Since the compound is crystallized to a high extent, the brittle morphology is as expected. This also gives material, a high melting or degradation temperature which is known as up to about 400°C .

The powder form SEM image of compound **2** was seen in Fig. 3. The powders were precipitated separately possibly due to the bonding difference. Since the N-H bonding has been exchanged by N- CH_3 , the intramolecular and intermolecular agglomeration may be difficult, as a result, individual precipitation may occur. The better the dissolution possibility can be said better the film characteristic.

The thick film morphology of compound **1** is seen in Fig. 4. As seen clearly, there are some places of agglomeration due to spin coating viscosity but by higher magnification, clear surfaces with drying cracks are evident. The coating quality is high and the roughness is seen as very low due to regular grain size distribution.

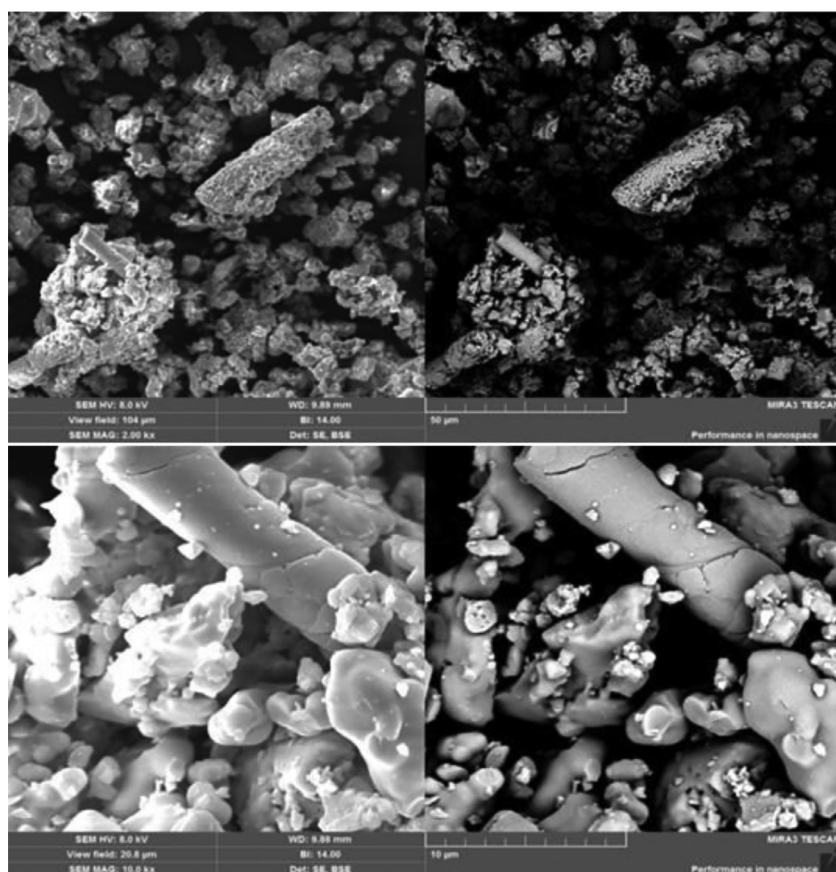


Fig. 3. SEM image of compound 2 and high magnified of powder as above.

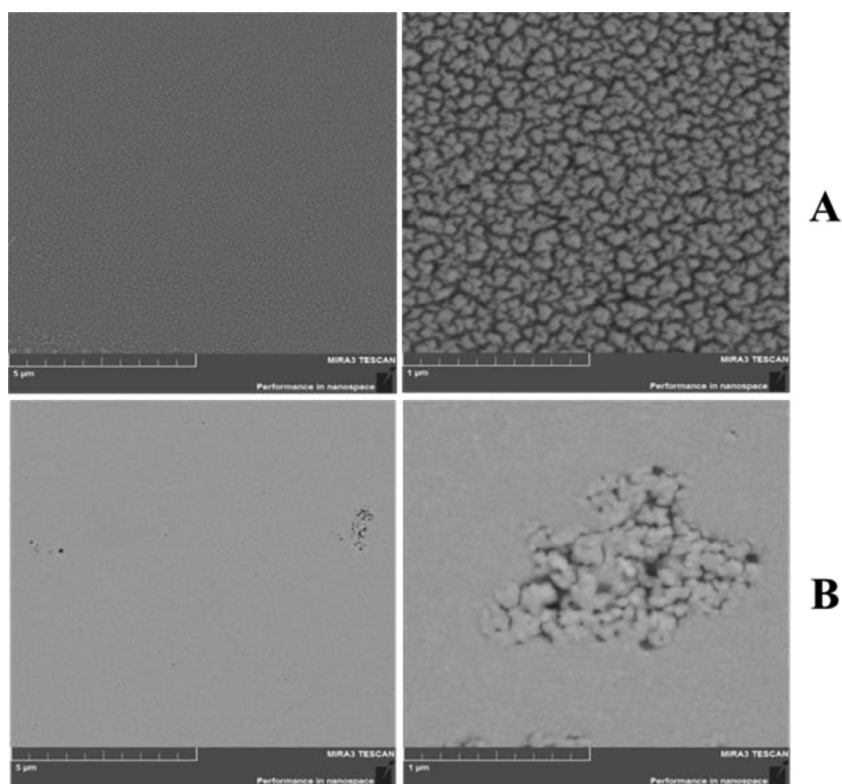


Fig. 4. Thick film characteristic of compound 1 (A) and compound 2 (B) with magnified views.

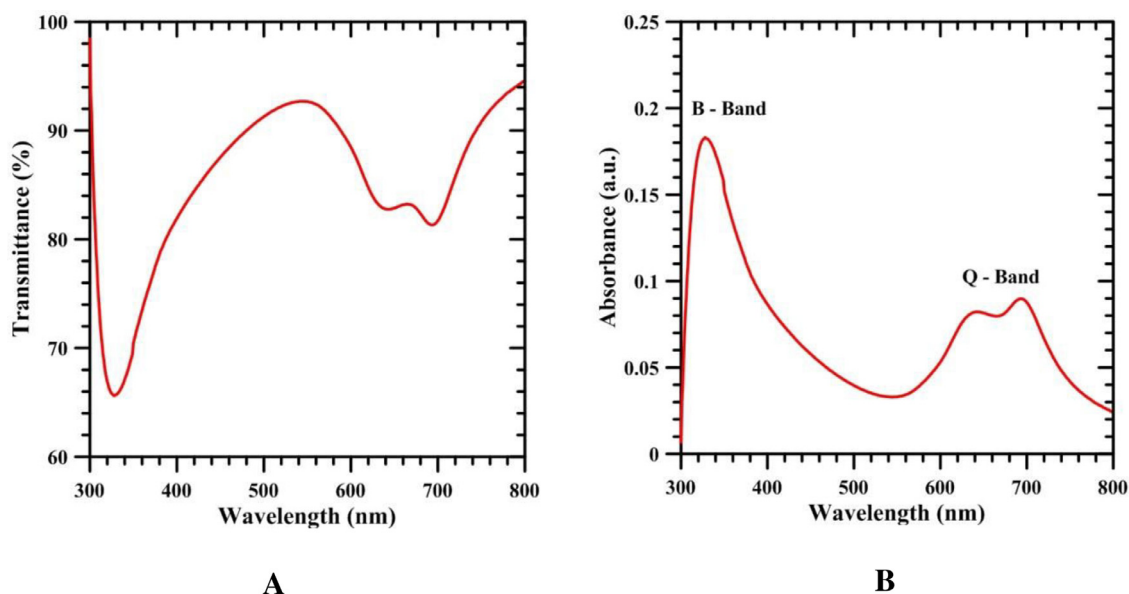


Fig. 5. The transmittance (A) and absorption (B) spectrum of compound 1 thin film.

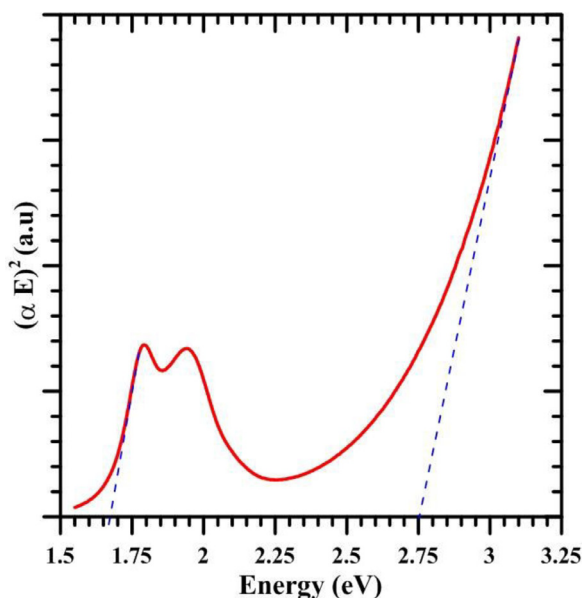


Fig. 6. Determination of the band gap of compound 1 thin film.

The films are very smooth and the interface between glass and compound **1** is very strong. Besides, films of compound **2** are also smooth but with some deficiencies as agglomeration compound **2**. It is thought that the dispersed and precipitated particles in compound **2** compared to compound **1** are attracted by high interaction energy and accordingly the molecules tend to stack. The interaction is thought to be a π - π stacking with van der Waals forces that will precipitate by interfering with film formation.

According to these results, we can say that thin films of compound **1** have the potential to be used to fabricate organic semiconductor devices.

3.3. Spectral properties

The study of optical properties is very important as they provide information about the electronic structures and optical transition types of a material [28]. There are two types of energy bands

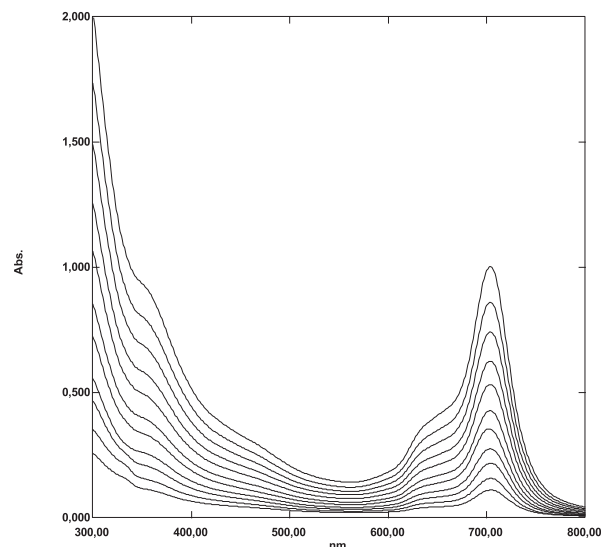


Fig. 7. UV-Vis spectra of compound 1 in different concentrations in DMSO.

(Q-band and B-band) of phthalocyanines, which show interesting optical properties due to their conjugated ring structure. The optical band gap was determined by UV-Vis spectroscopy of the thin film of compound **1**, which tends to form the smoothest thin film. In order to determine the optical properties of compound **1**, optical transmission and absorbance spectra of the thin film of the compound were taken in the wavelength range of 300–800 nm at room temperature (Fig. 5). The transmittance spectra of the compound **1** thin film revealed Q and B absorption bands around 620–720 nm and 328 nm, respectively. Both Q-band and B-band arise primarily due to the π - π^* transitions and the lowest allowed n - π^* transition might also be found in the B-band [29]. The transmittance value for compound **1** is above 80% in the visible region.

The optical band gap of compound **1** was determined from analysis of the absorption spectrum of the compound's thin film as described by the Tauc plot using the formula [5,30].

$$\alpha h\nu = \alpha_0(h\nu - E_g)^n$$

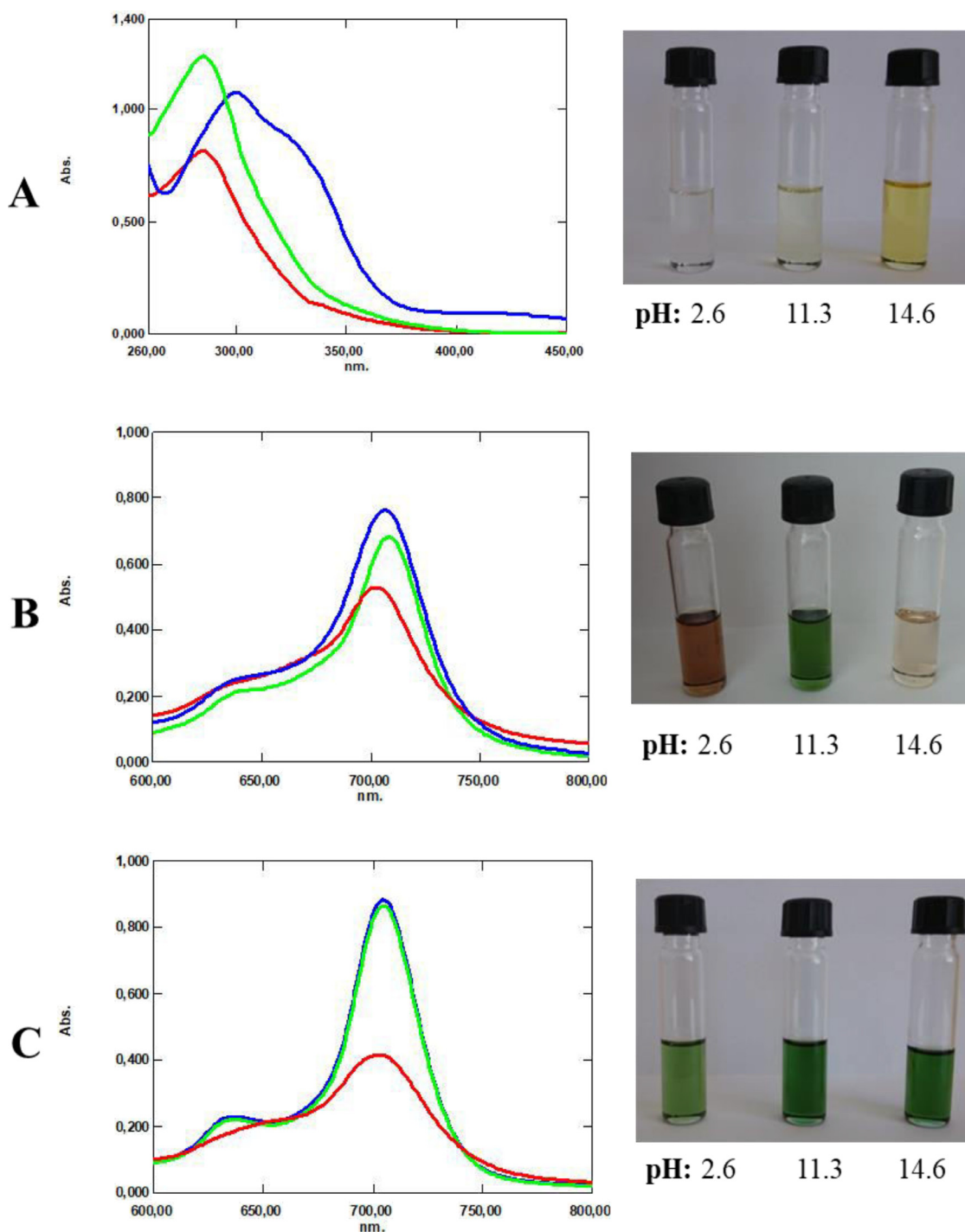


Fig. 8. pH-dependent UV-Vis spectra of (A) imidazole substituted phthalonitrile, (B) compound **1** and (C) compound **2** in DMSO ---[pH: 11.3 (–green), pH: 2.6 (–red), pH: 14.6 (–blue)].

where α is absorption coefficient, $h\nu$ is the energy of the incident photons and E_g is the value of the optical band gap energy (eV) corresponding to the transitions denoted by the n value. α_0 is a constant that depends on the transition probability. The best linear fit for semiconductors was found for $n = 0.5$, indicating the direct transitions allowed in the material [5,31,32].

The absorption coefficients were calculated using the absorption data using the equation given below [32].

$$\alpha = 1/d \ln(T)$$

where “ T ” is the transmittance of the thin film and “ d ” is the thickness of the film.

With UV-Vis spectroscopy, which is an easy and understandable technique to determine the E_g of organic π conjugated systems, and can be estimated according to the equation below [5].

$$E_g = 1242 / \lambda_{th}$$

where λ_{th} represents the threshold wavelength obtained from the beginning of the absorption spectrum [5].

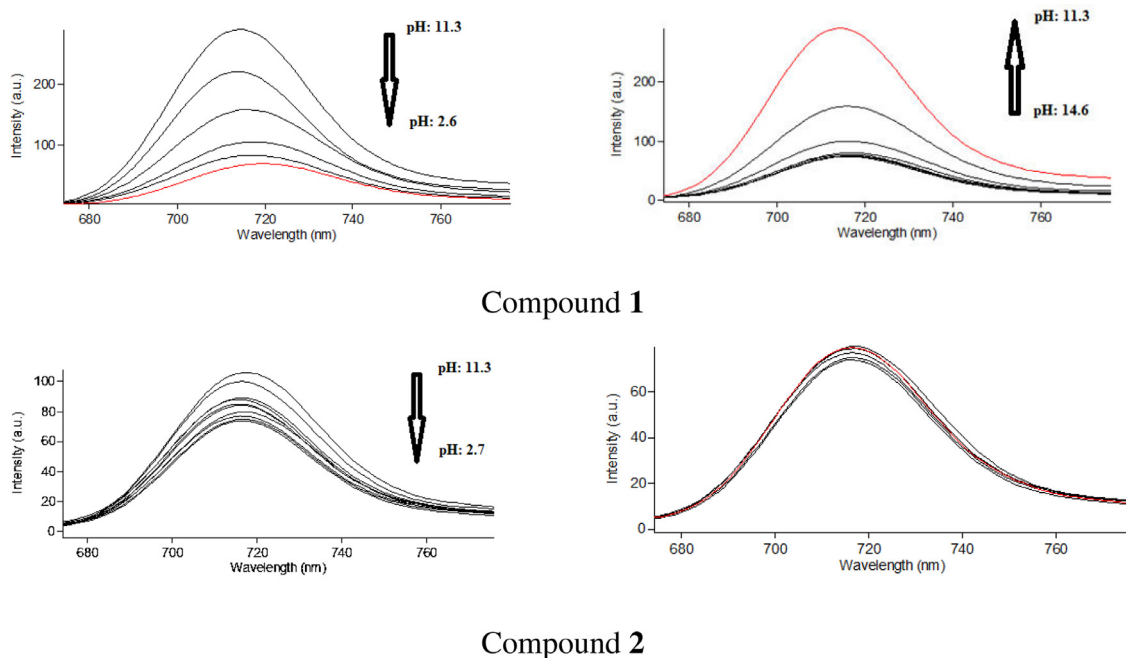


Fig. 9. pH-dependent fluorescence spectra of compounds **1** and **2** in DMSO.

As seen in Fig. 6, extrapolating the Tauc plot to the abscissa gives the value of the optical band gap [5]. According to the graph, the Q-band optical band gap of compound **1** was determined as 1.67 eV and the B-band optical band gap was determined as 2.75 eV which makes these films attractive for photovoltaic applications.

Aggregation of phthalocyanines depends on the solution concentration, the types of metal ions, the nature of the solvent, and the nature of the substituents [33,34]. It is desirable that phthalocyanines do not aggregate because it reduces energy efficiency in applications [33,35,36]. In this study, aggregation behavior of compounds **1**, **2** and **3** in different solvents (THF, DMF, DMSO) and different concentrations (in DMSO) was investigated with UV-Vis spectrophotometer in solution phase (Fig. 7). No significant aggregation was observed in any of the compounds **1-3**.

The fluorescent properties of compounds **1**, **2** and **3** in solution were studied. Fluorescence quantum yields were calculated from the measured emission spectra of compounds **1-3**. Fluorescent quantum yields of compounds can be used to explain energy transfers within the molecule [37]. The fluorescent quantum yields for compounds **1**, **2** and **3** are 0.51, 0.58 and 0.59, respectively, while this value is 0.18 [38] for unsubstituted ZnPc. It was observed that the fluorescence quantum yield increased significantly with the binding of the imidazole groups to the phthalocyanine ring and the modification of the alkyl groups to this molecule. Also, it is thought that the energy transfers between the substituted imidazole groups and the phthalocyanine ring may result in an increase in fluorescent quantum yields.

3.4. Colorimetric pH sensing properties

The pH dependent of compounds was investigated in DMSO solution by using UV-Vis spectrum. Spectroscopic pH studies were performed by using perchloric acid (HClO_4) and tetrabutylammonium hydroxide (TBAOH) to the solutions of the compounds in DMSO. pH values were measured with a glass electrode in electronic pH meter.

In Fig. 8, the color changes and UV-Vis spectral changes of imidazole substituted phthalonitrile, compound **1** and compound **2**

in acidic (pH: 2.6) and basic (pH: 11.3, 14.6) regions in DMSO are shown. Spectral changes are observed in the UV-Vis spectrum of compound **1** when treated with acid and base (Fig. 8B). The same effect is seen in the imidazole substituted phthalonitrile derivative (Fig. 8A). As seen in the UV-Vis spectrum of compound **2** (Fig. 8C), no spectral change is observed when treated with base. Compound **1** has spectral and color changes due to protonation and deprotonation in the acidic and basic regions, respectively, at the same time, the pH-dependent spectral responses and color transformations of compound **1** in the acidic and basic regions are reversible. Compound **2** has spectral and color changes only in the acidic regions, it does not show any change in the basic region. Accordingly, the pH-dependent spectral responses and color transformation of compound **2** are only reversible in the acidic region.

Emission spectra at different pHs for compounds **1** and **2** are shown in Fig. 9. As observed in the UV-Vis spectra, in the emission spectra of compound **1** were observed the changes due to protonation/deprotonation, while in the emission spectrum of compound **2** only observed the changes in the acidic region due to protonation.

In fact, in the first step of this study, pH-dependent colorimetric and spectral changes of compound **1** were observed. These changes were thought to result from the protonation/deprotonation of the substituted imidazole groups (Fig. 10) [15]. To prove this, we examined the same effect by blocking the nitrogen groups on the imidazole groups. Therefore, we synthesized compounds **2** and **3**. We saw that when the nitrogen atoms in substituted imidazole are capped with alkyl groups, the same effect could not be observed, because protonation/deprotonation could not occur. As the -NH group of substituted imidazole in compound **2** is alkylated, it was observed that it was affected only by acids. In compound **3**, it was observed that the substituted imidazole was not affected by acid and base since both -NH and -N groups were alkylated. This showed us that the spectral and color changes of compound **1** at acidic and basic pHs are due to the protonation/deprotonation mechanism of the substituted imidazole groups. As a result, it has been observed that compound **1** has colorimetric pH sensing properties and fluorescent-based “off-on-off” type molecular switch properties.

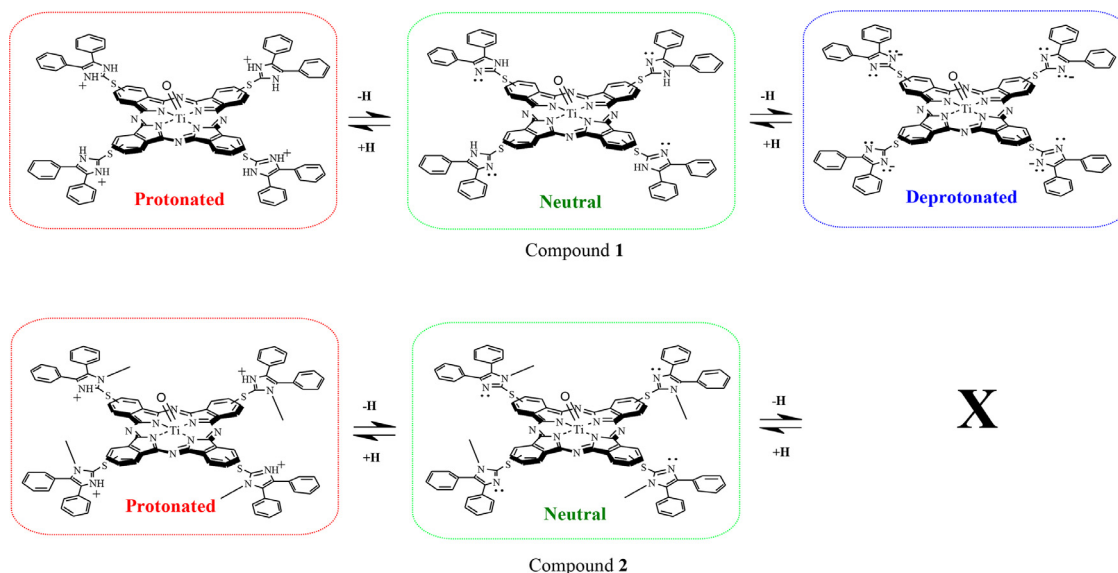


Fig. 10. Protonation/deprotonation of compounds 1 and 2. (X: no deprotonated)

4. Conclusions

In this study, imidazole substituted **1**, N-alkylated imidazole substituted **2** and water-soluble **3** oxo-titanium phthalocyanine compounds were synthesized and characterized. All of the synthesized compounds are soluble in organic solvents, and in addition, compound **3** is also soluble in water. The surface properties of compounds **1** and **2** in powder form and thin films were investigated by SEM. Compound **1** was observed to have a very smooth thin film structure in SEM images, thus it can be said that it has the potential to be used to fabricate semiconductor devices. The optical properties of compound **1** were studied (between 300 and 800 nm) in a UV-Vis spectrophotometer and the absorbance was recorded as a function of photon energy. The Q-band and B-band optical band gaps of compound **1** are determined as 1.67 eV and 2.75 eV, respectively. According to the optical band gap results, it can be said that compound **1** has the potential to be used in applications such as light emitting diode (LED), organic photovoltaic devices (OPV), and photodynamic therapy (PDT) as a photosensitizer. The fluorescent properties of the compounds were examined and the fluorescence quantum yields were calculated. Due to the increase in fluorescence quantum yields, it has been explained that there may be energy transfer between the substituted groups and the phthalocyanine ring. This result shows that the synthesized compounds may have the potential to be used in optical applications. The aggregation behavior of the synthesized compounds was also examined and no significant aggregation was observed. In addition, spectral and color changes of compounds **1-3** at different pHs were investigated. It was observed that compound **1** has a colorimetric pH sensor and fluorescent-based “off-on-off” type molecular switch properties.

Declaration of Competing Interest

The authors declare that they have no known competing financial interests or personal relationships that could have appeared to influence the work reported in this paper.

CRediT authorship contribution statement

Ebru Yabaş: Conceptualization, Methodology, Software, Validation, Formal analysis, Investigation, Resources, Writing – review & editing, Data curation, Visualization, Supervision.

Acknowledgment

In this study, the laboratory facilities of the Advanced Technology Application and Research Center (CÜTAM) of Sivas Cumhuriyet University were used. The author wish to thank Dr. Ali ÖZER for the SEM images.

References

- [1] A. Günsel, E. Kırbaç, B. Tüzün, A. Erdoğan, A.T. Bilgiçli, M.N. Yaraşır, Selective chemosensor phthalocyanines for Pd²⁺ ions; synthesis, characterization, quantum chemical calculation, photochemical and photophysical properties, *J. Mol. Struct.* 1180 (2019) 127–138.
- [2] N.B. McKeown, *Phthalocyanine Materials Synthesis, Structure and Function*, Cambridge University Press, 1998.
- [3] C.G. Claessens, W.J. Blau, M.J. Cook, M. Hanack, R.J.M. Nolte, T. Torres, D. Wöhrle, Phthalocyanines and phthalocyanine analogues: the quest for applicable optical properties, *Monatsh. Chem.* 132 (2001) 3–11.
- [4] A. Erdogmuş, M. Durmuş, A.L. Uğur, O. Avcıata, U. Avcıata, T. Nyokong, Synthesis, photophysics, photochemistry and fluorescence quenching studies on highly soluble substituted oxo-titanium(IV) phthalocyanine complexes, *Synth. Met.* 160 (2010) 1868–1876.
- [5] K.J. Hamam, M.I. Alomari, A study of the optical band gap of zinc phthalocyanine nanoparticles using UV-Vis spectroscopy and DFT function, *Appl. Nanosci.* 7 (2017) 261–268.
- [6] A.J. Beneto, V. Thiagarajan, A. Siva, A Tunable Ratiometric pH Sensor Based on Phenanthro[9,10-d]imidazole covalently linked with vinylpyridine, *RSC Adv.* (2013) 1–3.
- [7] N. Saleh, Y.A. Al-Soud, W.M. Nau, Novel fluorescent pH sensor based on coumarin with piperazine and imidazole substituents, *Spectrochim. Acta A* 71 (2008) 818–822.
- [8] F. Cheng, N. Tang, J. Chen, G. Chen, Luminescent pH sensor of a novel imidazole-containing hexanuclear Ru(II) polypyridyl complex, *Spectrochim. Acta A* 114 (2013) 159–163.
- [9] X. Chen, Z. Chen, B. Hu, P. Cai, S. Wang, S. Xiao, Y.L. Wu, X. Chen, Synergistic lysosomal activatable polymeric nanoprobe encapsulating pH sensitive imidazole derivative for tumor diagnosis, *Small* 14 (2018) 1703164–1703172.
- [10] F. Cheng, S. Yu, C. He, M. Ren, H. Yin, Two star-shaped tetranuclear Ru(II) complexes containing uncoordinated imidazole groups: synthesis, characterization, photophysical and pH sensing properties, *Luminescence* 31 (2016) 712–721.
- [11] F. Cheng, N. Tang, J. Chen, L. Chen, Proton-induced fluorescence switch of a novel hexanuclear Ru(II) polypyridyl complex containing imidazole ring, *Sens. Actuat. B-Chem.* 171–172 (2012) 102–109.
- [12] E. Yabaş, M. Sülü, S. Saydam, F. Dumludağ, B. Salih, Ö. Bekaroğlu, Synthesis, characterization and investigation of electrical and electrochemical properties of imidazole substituted phthalocyanines, *Inorg. Chim. Acta* 365 (2011) 340–348.
- [13] E. Yabaş, M. Sülü, F. Dumludağ, A.R. Özkaya, B. Salih, Ö. Bekaroğlu, Electrical and electrochemical properties of double-decker Lu(III) and Eu(III) phthalocyanines with four imidazoles and N-alkylated imidazoles, *Polyhedron* 42 (2012) 196–206.

- [14] E. Yabaş, M. Sülü, F. Dumludağ, B. Salih, Ö. Bekaroğlu, Imidazole octasubstituted novel mono and double-decker phthalocyanines: Synthesis, characterization, electrical and gas sensing properties, *Polyhedron* 153 (2018) 51–63.
- [15] S.Z. Topal, E. Önal, A.G. Gürek, C. Hirel, pH-induced “off-on-off” type molecular switch behaviors of zinc and free tetraimidazophthalocyanines, *Dalton Trans.* 42 (2013) 11528–11536.
- [16] X.F. Zhang, W. Guo, Imidazole functionalized magnesium phthalocyanine photosensitizer: modified photophysics, singlet oxygen generation and photooxidation mechanism, *J. Phys. Chem. A* 116 (2012) 7651–7657.
- [17] H.T. Akçay, R. Bayrak, Ü. Demirbaş, A. Koca, H. Kantekin, I. Degirmencioğlu, Synthesis, electrochemical and spectroelectrochemical properties of peripherally tetra-imidazole substituted metal free and metallophthalocyanines, *Dyes Pigm.* 96 (2013) 483–494.
- [18] H.T. Akçay, R. Bayrak, S. Karslıoğlu, E. Şahin, Synthesis, characterization and spectroscopic studies of novel peripherally tetra-imidazole substituted phthalocyanine and its metal complexes, the computational and experimental studies of the novel phthalonitrile derivative, *J. Organomet. Chem.* 713 (2012) 1–10.
- [19] X.F. Zhang, Y. Lin, W. Guo, J. Zhu, Spectroscopic insights on imidazole substituted phthalocyanine photosensitizers: Fluorescence properties, triplet state and singlet oxygen generation, *Spectrochim. Acta A* 133 (2014) 752–758.
- [20] B. Przybył, J. Janczak, Complexes of zinc phthalocyanine with monoaxially coordinated imidazole-derivative ligands, *Dyes Pigm.* 130 (2016) 54–62.
- [21] L. Dong, T. Xu, W. Chen, W. Lu, Synergistic multiple active species for the photocatalytic degradation of contaminants by imidazole-modified g-C₃N₄ coordination with iron phthalocyanine in the presence of peroxymonosulfate, *Chem. Eng. J.* 357 (2019) 198–208.
- [22] S. Bhattacharya, C. Biswas, S.S.K. Raavi, J.V.S. Krishna, D. Koteswar, L. Giribabu, S.V. Rao, Optoelectronic, femtosecond nonlinear optical properties and excited state dynamics of a triphenyl imidazole induced phthalocyanine derivative, *RSC Adv.* 9 (2019) 36726–36741.
- [23] B. Jamoussi, R. Chakroun, A. Timoumi, K. Essalah, Synthesis and characterization of new imidazole phthalocyanine for photodegradation of micro-organic pollutants from sea water, *Catalysts* 10 (2020) 906–926.
- [24] A. Günşel, P. Taslimi, G. Yaşa Atmaca, A.T. Bilgiçli, H. Pişkin, Y. Ceylan, A. Erdoğmuş, M.N. Yaraşır, İ. Gülçin, Novel potential metabolic enzymes inhibitor, photosensitizer and antibacterial agents based on water-soluble phthalocyanine bearing imidazole derivative, *J. Mol. Struct.* 1237 (2021) 130402–130414.
- [25] R. Chakroun, B. Jamoussi, B. Al-Mur, A. Timoumi, K. Essalah, Impedance spectroscopy and dielectric relaxation of imidazole substituted palladium(II) phthalocyanine (ImPdPc) for organic solar cells, *ACS Omega* 6 (2021) 10655–10667.
- [26] W.L.F. Armarego, C.L.L. Chai, Purification of Laboratory Chemicals, Fifth, Butterworth/Heinemann, Tokyo, 2003.
- [27] M. Durmuş, T. Nyokong, Photophysical and fluorescence quenching studies of benzyloxyphenoxy-substituted zinc phthalocyanines, *Spectrochim. Acta A* 69 (2008) 1170–1177.
- [28] R.C. Cherian, C.S. Menon, Preparation and characterization of thermally evaporated titanium phthalocyanine dichloride thin films, *J. Phys. Chem. Solid.* 69 (2008) 2858–2863.
- [29] M. Novotny, J. Bulir, A. Bensalah-Ledoux, S. Guy, P. Fitl, M. Vrnata, J. Lancok, B. Moine, Optical properties of zinc phthalocyanine thin films prepared by pulsed laser deposition, *Appl. Phys. A* 117 (2014) 377–381.
- [30] M.M. El Nhass, B.S. Sollman, B.S. Metwally, A.M. Farid, A.A.M. Farag, A.A.El Shazly, Optical properties of evaporated iron phthalocyanine (FePc) thin films, *J. Opt.* 30 (2001) 121–129.
- [31] H.J. Kim, J.W. Kim, H.H. Lee, B. Lee, J.J. Kim, Initial growth mode, nanostructure, and molecular stacking of a ZnPc:C60 bulk heterojunction, *Adv. Funct. Mater.* 22 (2012) 4244–4248.
- [32] S. Mobbakeri, Y. Akaltun, A. Özer, M. Kılıç, E.Ş. Tüzemen, E. Gür, Gallium oxide films deposition by RF magnetron sputtering; a detailed analysis on the effects of deposition pressure and sputtering power and annealing, *Ceram. Int.* 47 (2021) 1721–1727.
- [33] T. Nyokong, Effects of substituents on the photochemical and photophysical properties of main group metal phthalocyanines, *Coord. Chem. Rev.* 251 (2007) 1707–1722.
- [34] T. Nyokong, Electronic spectral and electrochemical behavior of near infrared absorbing metallophthalocyanines, *Struct. Bond.* 135 (2010) 45–88.
- [35] C.C. Leznoff, A.B.P. Lever, Phthalocyanines Properties and Applications. Vol. 1, VCH Publisher, Cambridge, 1989.
- [36] H. Yalazan, K. Tekintas, V. Serdaroglu, E. Tugba Saka, N. Kahrman, H. Kantekin, Design, syntheses, spectroscopic, aggregation properties of novel peripheral octa-substituted zinc(II), magnesium(II) and lead(II) phthalocyanines and investigation of their photocatalytic properties on the photooxidation of 4-nitrophenol, *Inorg. Chem. Commun.* 118 (2020) 107998–108005.
- [37] K.M. Nimith, M.N. Satyanarayan, G. Umesh, Enhancement in fluorescence quantum yield of MEH-PPV:BT blends for polymer light emitting diode applications, *Opt. Mater.* 80 (2018) 143–148.
- [38] M. Durmuş, T. Nyokong, Photophysical and fluorescence quenching studies of benzyloxyphenoxy-substituted zinc phthalocyanines, *Spectrochim. Acta A* 69 (2008) 1170–1177.